Journal of Alloys and Compounds 615 (2014) S90–S92

Contents lists available at ScienceDirect

Journal of Alloys and Compounds

journal homepage: www.elsevier.com/locate/jalcom

Exploring the mechanical size effects in $Zr_{65}Ni_{35}$ thin film metallic glasses

Matteo Ghidelli [a,b,c], Antoine Volland [a], Jean-Jacques Blandin [a], Thomas Pardoen [b], Jean-Pierre Raskin [c], Frédéric Mompiou [d], Philippe Djemia [e], Sébastien Gravier [a,*]

[a] Science and Engineering of Materials and Processes, SIMaP, Grenoble University/CNRS, UJF/Grenoble INP, 101 rue de la physique, BP46, 38402 Saint-Martin d'Hères, France
[b] Institute of Mechanics, Materials and Civil Engineering, IMMC, Université catholique de Louvain, B-1348 Louvain-la-Neuve, Belgium
[c] Institute of Information and Communication Technologies, Electronics and Applied Mathematics, ICTEAM, Université catholique de Louvain, B-1348 Louvain-la-Neuve, Belgium
[d] CEMES-CNRS, Université de Toulouse, 29, rue J. Marvig, 31005 Toulouse, France
[e] LSPM-CNRS, Université de Paris 13, Sorbonne Paris Cité, F-93430 Villetaneuse, France

ARTICLE INFO

Article history:
Available online 1 December 2013

Keywords:
Metallic glasses
Thin films
Vapor deposition
Mechanical properties
Size effects

ABSTRACT

Mechanical size effects in $Zr_{65}Ni_{35}$ Thin Film Metallic Glass (TFMG) are studied with an emphasis on a transition in failure mechanisms occurring below 500 nm. XRD and TEM analyses of $Zr_{65}Ni_{35}$ TFMG confirm the absence of a crystalline phase. The thickness effect on the mechanical properties of $Zr_{65}Ni_{35}$ TFMGs is investigated using nanoindentation, Brillouin spectroscopy, and fracture tests. Brillouin spectroscopy shows no variation of the elastic constants, while the hardness – measured by nanoindentation – presents a continuous increase with decreasing film thickness. The fracture surface of the TFMGs involves corrugations which disappear when the thickness is reduced below 500 nm.

1. Introduction

The trend in industry towards miniaturization does not only apply to microelectronics, but also to domains like micromechanics, optics and medical science. In the case of crystalline materials, there are many difficulties in predicting the mechanical response when the size of the system becomes close to the internal length scale of the microstructure (such as the grain size in polycrystalline materials), impacting the design of reliable systems [13,1]. Compared with conventional crystalline MEMS materials, TFMGs have structural advantages among which high rupture strength or large elastic deformation ability, owing to their disordered atomic structure [5]. Furthermore, crystalline materials are limited because of the stress gradient that usually hinders their possibility to be released from the substrate without bending, like in the case of cantilever folding [15]. The physical properties of metallic glasses can be tuned and mechanical properties can be enhanced by changing their compositions as well as by the precipitation of nanoscale particles [18]. As a consequence, TFMGs are good candidates for micro-components fabrication. Nevertheless, several recent works have shown that their mechanical behavior might depend on the dimension of the tested samples as for their crystalline counterparts [20,21]. Micropillar compression tests suggest that, when the size of the sample is reduced below a few micrometers, the deformation is localized in shear bands [9,10] as for bulk samples, but with enhanced plasticity. When the size of the sample is further reduced, another deformation regime is observed in which metallic glass can deform plastically with no direct evidence of shear banding [3]. Nevertheless, while this technique has the advantages to be intuitive and easy to perform, it shows several drawbacks and especially the Ga-ions surface damaging, when prepared by focused ion beam (FIB) [8]. As a consequence, a monotonic trend of the main mechanical properties with the reduction of the pillar diameter has not been demonstrated yet and controversy still exists about a transition of deformation mode from inhomogeneous, with shear bands formation, to homogeneous [4,19].

TFMGs hence are interesting as potential materials for microelectronics, but they also represent an alternative way avoiding FIB milling to investigate size effects in metallic glasses. Here, we present a study of elastic constants, hardness and fracture surface analysis as a function of the thickness in the case of $Zr_{65}Ni_{35}$ TFMGs.

2. Experimental

$Zr_{65}Ni_{35}$ (at.%) TFMGs have been deposited with thicknesses from 300 up to 900 nm on a cleaned Si (1 0 0) substrate by means of DC-Magnetron sputtering (Alliance Concept AC450) within a clean room (class 1000) to limit sample contamination. In order to limit impurity contents and to control the film stoichiometry, a composite sputtering target was designed consisting of pure grade Ni rectangular slices inserted into a pure Zr matrix. The composition of the film has been checked by energy dispersive X-ray spectroscopy (EDX) and electron probe micro analysis

* Corresponding author. Tel.: +33 (0)476826379.
E-mail address: sebastien.gravier@simap.grenoble-inp.fr (S. Gravier).

0925-8388/$ - see front matter © 2013 Elsevier B.V. All rights reserved.
http://dx.doi.org/10.1016/j.jallcom.2013.11.154

(EPMA) and found to be close to $Zr_{65}Ni_{35}$ with a negligible amount of C and O, whatever the position on the silicon substrate. The film atomic structure was investigated by X-ray diffraction (XRD, Cu Kα radiation) using a grazing incidence geometry to avoid Si substrate signal. The results were consolidated by cross-section transmission electron microscopy (TEM – CM20 FEG operating at 200 kV). The elastic constants have been determined using the Brillouin light scattering (BLS) technique, see [6] for details. The hardness has been measured by nanoindentation with a diamond Berkovich tip mounted on an Agilent G200 Nanoindenter DCM II head. The force and vertical displacement resolutions are ~50 nN and ~0.01 nm, respectively. Prior to the beginning of tests, the tip area function was calibrated using a fused silica reference. The nanoindentation measurements were performed under a load-control mode at room temperature. The allowable thermal drift rate has been limited to 0.05 nm s^{-1}. Sixteen indents were made within each sample for statistical analysis and consistency inspection. The measurements were carried out using the continuous stiffness measurements (CSM) technique providing the continuous hardness with increasing indentation depth with a constant loading rate imposed equal to 0.05 s^{-1}. The hardness was calculated using the Oliver–Pharr method [12].

3. Results and discussion

Fig. 1 shows the X-ray diffractograms of $Zr_{65}Ni_{35}$. As expected in the case of amorphous samples, two broad halos are present centered at 37° and 63°, respectively. Diffractograms involve the same shape whatever the thickness, indicating a similarity in the atomic structure for all TFMGs. In order to further confirm the amorphous structure of the films, TEM electron micro-diffraction is reported in Fig. 1 inset for a 900 nm-thick film showing no atomic periodicity as inferred from the presence of diffuse haloes. Fig. 2 reports the values corresponding to the Young's modulus and the Poisson ratio as a function of the thickness of the TFMG. A constant value of the Young's modulus equal to ~71 GPa is found whatever the thickness of the TFMG. This value is in relatively good agreement with the value reported by Ristić et al. [16] and Dong et al. [7] who found an elastic modulus equal to 65 GPa for ZrNi ribbons. Furthermore, Poisson ratio equal to 0.39 is found, independent of the film thickness. Those trends show that the elastic constants do not depend on the thickness and are an additional proof that the local atomic environment is the same for all thicknesses.

The hardness of the films has been directly calculated on the rough curve as a function of the indentation depth. In general, the hardness of a thin film is considered independent from the underlying substrate as long as the penetration depth is shallow enough, namely when the normalized indentation depth (corresponding to the indentation depth divided by the TFMG thickness) is smaller than a critical value. This critical value is mainly dependent on the stiffness and strength ratio between the film and substrate [17]. For films deposited on a stiff and hard substrate, the "10% of film thickness" rule of thumb is generally valid for the critical penetration. The evolution of the hardness as a function of the normalized indentation depth is given in Fig. 3a for $Zr_{65}Ni_{35}$

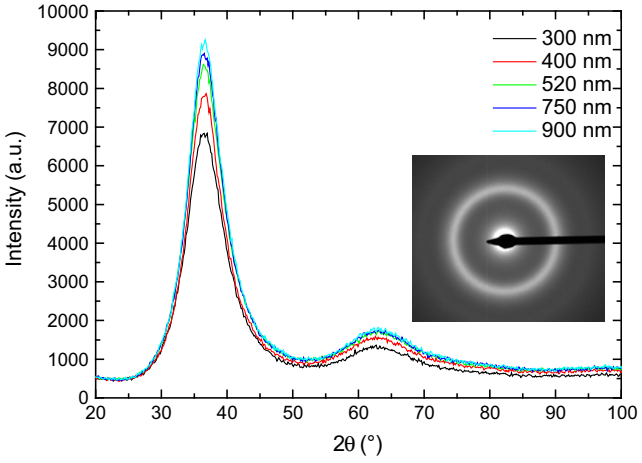

Fig. 1. XRD diffractograms of $Zr_{65}Ni_{35}$ TFMGs with different thicknesses. A first sharp diffraction peak and a second broader peak at higher θ angles are observed, respectively, around 37° and 63°. In the inset, TEM micro diffraction pattern for the 900 nm-thick film showing two diffuse haloes, further proving the film's amorphous structure.

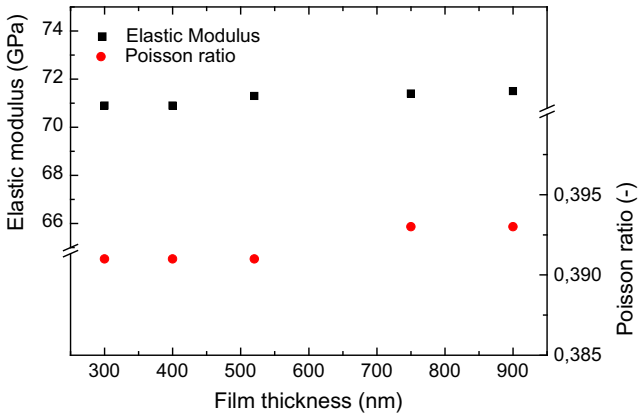

Fig. 2. Evolution of the Young's modulus and poisson ratio as function of the thickness for $Zr_{65}Ni_{35}$ TFMGs. Both values are found independent on film thickness and equal to 71 GPa and 0.39, respectively.

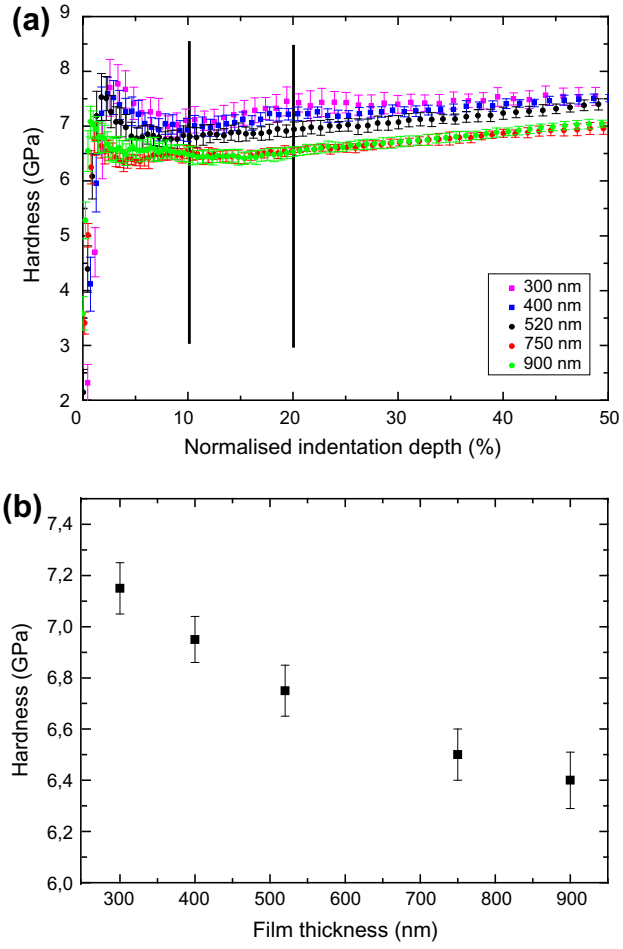

Fig. 3. (a) Hardness as function of normalized indentation depth for $Zr_{65}Ni_{35}$ TFMGs with different thicknesses, vertical back lines represent the region in which film average hardness has been extracted. (b) Average hardness variation with the film thickness for $Zr_{65}Ni_{35}$ TFMGs on silicon substrate.

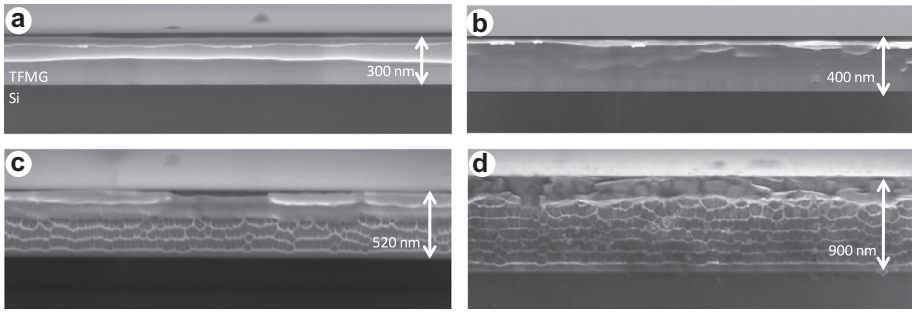

Fig. 4. SEM fracture surface of $Zr_{65}Ni_{35}$ TFMGs with different thicknesses from (a) to (d), respectively, 300 nm, 400 nm, 520 nm and 900 nm. In all samples, the Si substrate is located at the bottom part of the image. A corrugation pattern is visible only starting from 500 nm.

TFMGs with different thicknesses. We note that there is a large plateau to which the indentation test produces substrate independent hardness measurements (black vertical lines in Fig. 3a) [17]. As a consequence, the extracted average hardness values (Fig. 3b) are not affected by the artefact bump found at low normalized indentation depth (Fig. 3a) as well as by substrate effects.

Fig. 3b shows the variation of the hardness as a function of the film thickness. The hardness increases with decreasing film thickness from 6.4 to 7.2 GPa for the 900–300 nm-thick film, respectively. Experimental results have shown an increase of the yield stress when reducing the sample size [20,9]. Note that Ristić et al. [17] reported values of around 5.2 GPa for $Zr_{65}Ni_{35}$ metallic glass ribbons obtained using micro-hardness measurements, even if it has been demonstrated that the hardness is dependent on the applied load [15]. This general trend indicates a moderate "size effect" associated to the plastic deformation mechanism. But, an important point here is that the size effect remains present when the hardness is compared at the same indentation depth (within the substrate independent regime) and thus at the same indentation volume for different film thicknesses. This might indicate another source of size dependency linked to the film thickness. The origins of this effect is still under investigation.

Lastly we investigated the fracture mechanisms. Fracture tests on TFMGs were addressed by cleaving both the substrate and the TFMG, and observing the fracture surface by Scanning Electron Microscope (SEM). Fig. 4 shows micrographs with various fracture surfaces depending on the film thickness. In all samples, a clear interface separates the Si substrate (corresponding to the darker bottom region) from the thin film. A transition in the fracture morphology respectively for thin ($\leqslant$400 nm) and large ($\geqslant$500 nm) thicknesses is observed. The formers show a uniform surface characterized only by a top folded part, whereas in the latter a corrugation pattern covers around 2/3 of the film thickness leaving a folded layer in the proximity of the top surface, likewise the thinnest films (see for instance the 520 nm-thick sample, Fig. 3c). The dimple structure has features similar to other BMGs fractured under compressive stress [2,23]. The small scale of the corrugations (below 200 nm) is close to values reported by [22,11] for brittle metallic glasses. According to Xi et al. [22], the corrugation size is linked to the plastic zone at the crack tip, thus a nm-scale dimple structure indicates a low fracture toughness.

4. Conclusion

In order to follow an alternative route to address mechanical size effect in metallic glasses, various thicknesses of $Zr_{65}Ni_{35}$ thin films were deposited by DC magnetron sputtering. The amorphous structure was checked by XRD and TEM. The elastic constants were obtained by Brillouin spectroscopy and do not show any variations with thickness, providing no evidence of atomic structural change reducing film thickness. On the other hand, it is shown that there is an evolution of the plastic and fracture behaviors. Indeed, a moderate increase of the hardness is detected when the thin film thickness is decreased. Moreover, thorough observations of the fracture surfaces of TFMGs were performed for different thicknesses pointing out a morphological transition, in which a corrugation pattern is visible above 500 nm, while a mirror-like surface appears for thinner films. A deeper analysis is in progress to understand and model this transition.

Acknowledgments

The authors would like to thanks the IDS-FunMat for the PhD funding, the ANR MEGAPROSE project no. JC08 314226 for its financial support. Thin film preparation was performed with the help of the "Plateforme Technologique Amont" (Grenoble, France), and with the financial support of the Nanosciences Fundation and CNRS Renatech network.

References

[1] N. Andre, M. Coulombier, V. De Longueville, D. Fabregue, T. Gets, S. Gravier, T. Pardoen, J.-P. Raskin, Microelectron. Eng. 84 (2007) 2714–2718.
[2] V.Z. Bengus, E.D. Tabachnikova, J. Miskuf, K. Csach, V. Ocelík, W.L. Johnson, V.V. Molokanov, J. Mater. Sci. 35 (2000) 4449–4457.
[3] C.Q. Chen, Y.T. Pei, J.T.M. De Hosson, Acta Mater. 58 (2010) 189–200.
[4] C.Q. Chen et al., Phys. Rev. B: Condens. Matter. 83 (2011) 180201(R).
[5] J.P. Chu et al., Thin Solid Films 520 (2012) 5097.
[6] P. Djemia, F. Ganot, P. Moch, V. Branger, P. Goudeau, J. Appl. Phys. 90 (2001) 756.
[7] Y.D. Dong, G. Gregan, M.G. Scott, J. Non-Cryst. Solids 43 (1981) 403.
[8] Y.H. Lai, C.J. Lee, Y.T. Cheng, H.S. Chou, H.M. Chen, X.H. Du, C.I. Chang, J.C. Huang, S.R. Jian, J.S.C. Jang, T.G. Nieh, Scripta Mater. 58 (2008) 890–893.
[9] C.J. Lee, J.C. Huang, T.G. Nieh, Appl. Phys. Lett. 91 (2007) 161913.
[10] M.C. Liu, J.C. Huang, H.S. Chou, Y.H. Lai, C.J. Lee, T.G. Nieh, Scripta Mater. 61 (2009) 840–843.
[11] S.V. Madge et al., Acta Mater. 60 (2012) 4800.
[12] W.C. Oliver, G.M. Pharr, J. Mater. Res. 19 (2003) 3.
[13] B.C. Prorok, Y. Zhu, H.D. Espinosa, Z. Guo, Z.P. Bazant, Y. Zhao, B.I. Yakobson, in: H.S. Nalwa (Ed.), Micro-and Nanomechanics, Encyclopedia of Nanoscience and Nanotechnology, vol. 5, pp. 555–600.
[14] U. Ramamurty, S. Jana, Y. Kawamura, K. Chattopadhyay, Acta Mater. 53 (2005) 705–717.
[15] J.-P. Raskin, F. Iker, N. Andre, B. Olbrechts, T. Pardoen, D. Flandre, Electrochim. Acta 52 (2007) 2850–2861.
[16] R. Ristić, M. Stubičar, E. Babić, Philos. Mag. 87 (2007) 5629.
[17] R. Saha, W.D. Nix, Acta Mater. 50 (2002) 23.
[18] C.A. Schuh et al., Acta Mater. 55 (2007) 4067.
[19] Z.W. Shan et al., Phys. Rev. B: Condens. Matter. 77 (2008) 155419.
[20] L. Tian et al., Nature Commun. 3 (2012) 609, http://dx.doi.org/10.1038/ncomms1619.
[21] C.A. Volkert, A. Donohue, F. Spaepen, J. Appl. Phys. 103 (2008) 083539.
[22] X.K. Xi et al., Phys. Rev. Lett. 94 (2005) 125510.
[23] Z.F. Zhang, J. Eckert, L. Schultz, Acta Mater. 51 (2003) 1167–1179.